TELKOMNIKA, Vol. 11, No. 6, June 2013, pp. 3020 ~ 3027
e-ISSN: 2087-278X

Integrated Control of Nonlinear Vehicle Stability

Jie Tian[*1], Yaqin Wang[1], Ning Chen [2]
[1]College of Automobile & Traffic Engineering, Nanjing Forestry University, Nanjing, 210037, P.R.China
[2]College of Electro-Mechanical Engineering, Nanjing Forestry University, P.R.China
Corresponding author, e-mail: njtianjie@163.com*, secondsmile.happy@163.com, chenning@njfu.com.cn

Abstract

A novel vehicle stability control method integrated direct yaw moment control (DYC) with active front steering (AFS) is presented in this paper. By the phase plane of sideslip angle and sideslip angular velocity, vehicle stable region is determined. When the vehicle is outside the stable region, DYC controller is firstly used to produce proper direct yaw moment, which can make the vehicle back to the stable region. Then AFS controller of sliding mode variable structure is constructed and used to control the front steering angle of the actual vehicle, so that the sideslip angle and yaw rate of the actual vehicle model can track those of the reference vehicle model. Computer simulations are carried out on a 2-DOF nonlinear vehicle model to investigate the effectiveness of the proposed method. And the simulation results show that the influence of the proposed method on enhancing vehicle stability is significant.

Keywords: *nonlinear vehicle stability control, direct yaw moment control, active front steering, phase plane method, integrated control*

1. Introduction

Stability is an extremely important characteristic of a vehicle. According to the statistics, most of the high speed traffic accidents were caused by the lateral buckling. There are many control systems to improve the vehicle stability, such as four wheel steering system (4WS), steer-by-wire system (SBW), active front steering system (AFS), anti-lock braking system (ABS), traction control system (TCS), electric stability program (ESP), direct yaw moment control system (DYC) and so on [1].

In the above mentioned control systems, there are basically two methods to control yaw moment which is the most efficient way to improve vehicle stability. The first method is AFS, a kind of indirect yaw moment control, which works based on the control of the tire lateral force through steering angle control. The other method is DYC, in which an unequal distribution of tire longitudinal forces (mainly braking forces) produces a compensating external yaw moment [2]. Related studies show that AFS can produce an additional front steering angle and makes the actual value smaller in the over-steering condition, which can ensure that the yaw rate and sideslip angle perfectly track those of the reference vehicle model. While in the under-steering condition, the additional front steering angle produced by AFS makes the front steering angle too large, even beyond the allowed maximum angle of the steering mechanism, so the control effect of AFS is not ideal at this time [3]. In addition, tires prone to nonlinear saturation in the large corner and high-speed conditions, and it is difficult to change the under-steering characteristics of the vehicle through increasing of the front steering angle [4]. While at this time the control effect of DYC is very good [5, 6]. That is to say that the AFS performance is limited in the non-linear vehicle handling region. On the other hand, in spite of a good performance of DYC in both the linear and non-linear vehicle handling regions, continued DYC activation could lead to uncomfortable driving conditions and an increase in the stopping distance in the case of emergency braking. It is recommended that DYC be used only in high-g critical maneuvers [2]. Therefore, how to integrate AFS with DYC and make good use of their respective advantages to improve vehicle stability has become a hot spot for today's automotive research. And a novel integrated control is proposed in this paper.

The rest of the paper is organized as follows. The control strategy is stated and both of the reference and the actual vehicle models are given in Section 2. In Section 3, we discuss the determination of the stable region based on phase plane method and the design of DYC

Received January 5, 2013; Revised March 15, 2013; Accepted April 12, 2013

controller. In Section 4, we present the design of AFS controller based on sliding mode variable structure. The DYC and AFS controller are later used on the actual vehicle as discussed in Section 5 to demonstrate that the integrated controller is efficient. Finally, some concluding remarks are given in Section 6.

2. Problem Description

The main idea of DYC and AFS integrated control is as follows. Firstly, the stable region of the sideslip angle and sideslip angular velocity is determined based on the phase plane method. When the vehicle is outside the stable region, DYC controller is adopted to make the vehicle back to the stable region and improve the tire nonlinear saturation. Because the vehicle inside the stable region can be regarded as a linear model, AFS controller based on the linear vehicle model is adopted to generate an additional front steering angle, and to ensure that the sideslip angle and yaw rate is perfectly tracking the reference vehicle model. The concrete control block diagram is shown in Figure 1.

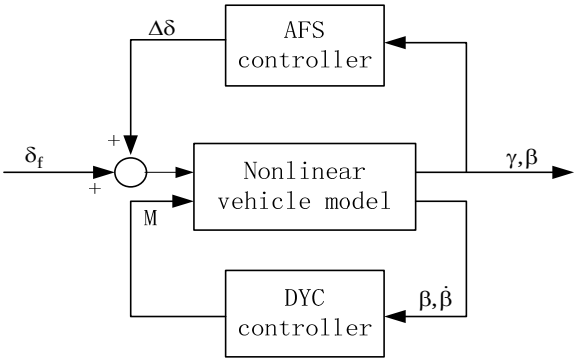

Figure 1. Integrated Control Block Diagram

2.1. Nonlinear Vehicle Model

The nonlinear vehicle is represented by the single track model which assumes front (rear) tires to be replaced by a single imaginary tire in the middle, which are then joined together with an imaginary weightless rod. The vehicle model is described as [7, 8]:

$$\begin{cases} mu(\dot{\beta}+\gamma) = F_f + F_r \\ I_Z\dot{\gamma} = l_f F_f - l_r F_r \end{cases} \tag{1}$$

The nonlinear tire characteristic is considered to capture the essential vehicle dynamics and to design the controller. In this paper the Pacejka tire model is used. According to its general expression, F_f (F_r) can be described as:

$$\begin{cases} F_f = D_f \sin\left\{C_f \arctan\left[B_f\alpha_f - E_f\left(B_f\alpha_f - \arctan(B_f\alpha_f)\right)\right]\right\} \\ F_r = D_r \sin\left\{C_r \arctan\left[B_r\alpha_r - E_r\left(B_r\alpha_r - \arctan(B_r\alpha_r)\right)\right]\right\} \end{cases} \tag{2}$$

Where m is the mass of the vehicle, I_z is the moment of inertia with respect to the vertical axis through the center of gravity (CG), β is the sideslip angle, γ is the yaw rate, u is the vehicle longitudinal velocity, which we hereafter refer to as the vehicle speed, l_f (l_r) is the distance from the front (rear) axle to the CG, F_f (F_r) is the cornering force of the front (rear) wheel, given by Pacejka tire mode, α_f (α_r) is the front (rear) sideslip angle, B_f (B_r), C_f (C_r), D_f (D_r) and E_f (E_r) are respectively the front (rear) stiffness factor, shape factor, peak factor and bulking factor of the front (rear) tire lateral force-sideslip angle curve.

The vehicle in reference [9] is debated here. And the tire model parameters of B, C, D, E with μ = 0.8, 0.2 are respectively as the Table 1. According to the Equation (2), the characteristic curves of the front and rear tire cornering force can be obtained by MATLAB, as illustrated in Figure 2.

Table 1. Parameters of Tire Model

Adhesion Coefficient	Tire	B	C	D	E
μ=0.8	Front	6.7651	1.20	-6426.8	-1.9990
μ=0.8	Rear	9.0051	1.20	-5420.0	-1.7908
μ=0.2	Front	11.275	1.56	-2574.7	-1.9990
μ=0.2	Rear	18.621	1.56	-1749.7	-1.7908

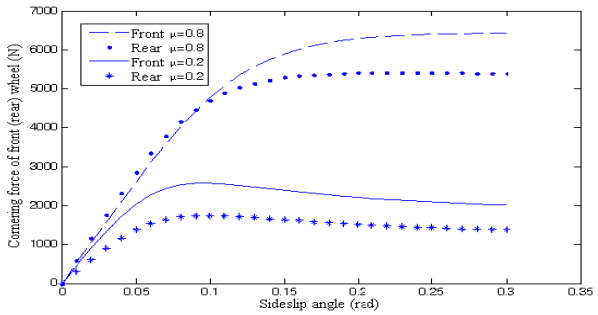

Figure 2. Characteristic Curves of the Tire Cornering Force

Figure 2 shows that the tires can be considered to be rigid when the sideslip angle is small. The front (rear) tire cornering stiffness with μ = 0.8, 0.2 can be respectively calculated by the linear part of the front (rear) tire cornering force characteristic curve. And the linear vehicle model can be described as the state-space representation of a linear time-invariant system with one input (δ_f , front steering angle) and two outputs (β and γ), and is given below:

$$\begin{cases} \dot{x} = Ax + Bu \\ y = Cx + Du. \end{cases} \tag{3}$$

2.2. Reference Vehicle Model

Here we consider the single track vehicle model with linear tire characteristic and neutral steering characteristic as the reference vehicle model. That is to adjust the distance from the front axle and the rear axle to the CG with the same wheelbase. And its model can be described as:

$$\begin{cases} \dot{x}_d = A_d x_d + B_d u_d \\ y_d = C_d x_d + D_d u_d. \end{cases} \tag{4}$$

$$x_d = \begin{pmatrix} \beta \\ \gamma \end{pmatrix}, u_d = \delta_f, A_d = \begin{pmatrix} (k_f + k_r)\frac{1}{mu} & (k_f l_f - k_r l_r)\frac{1}{mu^2} - 1 \\ (l_f k_f - l_r k_r)\frac{1}{I_z} & (k_f {l_f}^2 + k_r {l_r}^2)\frac{1}{I_z u} \end{pmatrix}, B_d = \begin{pmatrix} -k_f \frac{1}{mu} \\ -l_f k_f \frac{1}{I_z} \end{pmatrix}, C_d = \begin{pmatrix} 1 & 0 \\ 0 & 1 \end{pmatrix}, D_d = \begin{pmatrix} 0 \\ 0 \end{pmatrix}.$$

Where x_d is the measurable state, u_d is the front steering input, K_f (K_r) is the cornering stiffness of the front (rear) wheel, l_f (l_r) is substituted by the parameter of the reference vehicle.

3. Design of DYC Controller

There are two categories of vehicle stability control. One is to the trajectory maintaining which is described by sideslip angle. And the other is stability problem which is described by

yaw rate. But they are interrelated with each other and the stability problem is more important. Loss of stability means that it is difficult to restore to the stable region again. So usually too large sideslip angle does not allowed. When the sideslip angle is small, the vehicle which loses stability has no need to be controlled. While a large sideslip angel occurs, an indirect control is needed to change the increasing trend of the sideslip angle. Therefore, it is very important to determine the stable region.

3.1. Determination of the Stable Region based on Phase Plane Method

Taking into account that phase plane method is one of the common methods for analysis of a nonlinear system, we use it to determine the stable region. The present studies show that there are two kinds of the vehicle phase plane [10]: sideslip angle and yaw rate stable region, sideslip angle and sideslip angular velocity stable region.

Related studies have shown that the latter is superior to the former, so we select the latter as the basis for the determination of the stable region. The stable regions with different front steering angle (δ_f), different vehicle speed (v) and different road adhesion coefficients (μ) can be respectively obtained by MATLAB, as shown in Figure 3~8.

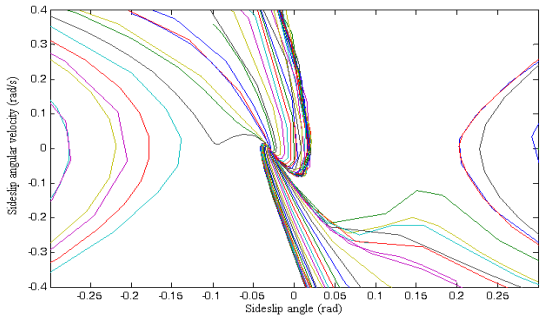

Figure 3. δ_f = 0.04rad, v=60km/h, μ=0.8

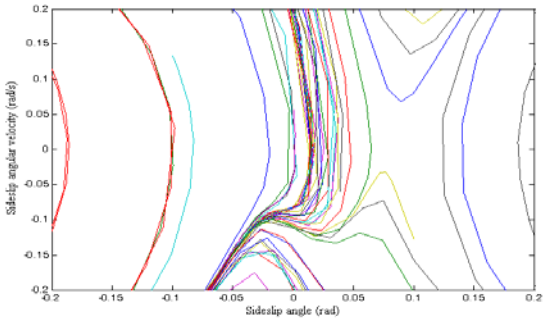

Figure 4. δ_f =0.04rad, v=60km/h, μ=0.2

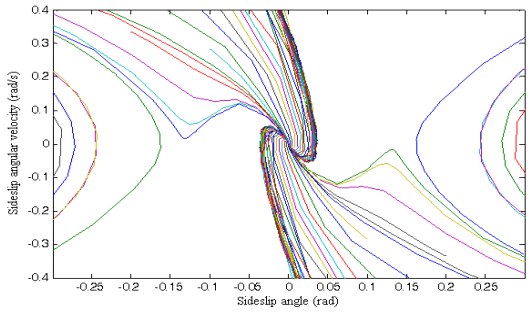

Figure 5. δ_f = 0rad, v=80km/h, μ=0.8

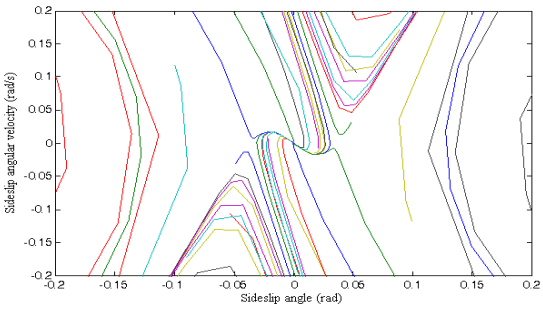

Figure 6. δ_f = 0rad, v=80km/h, μ=0.2

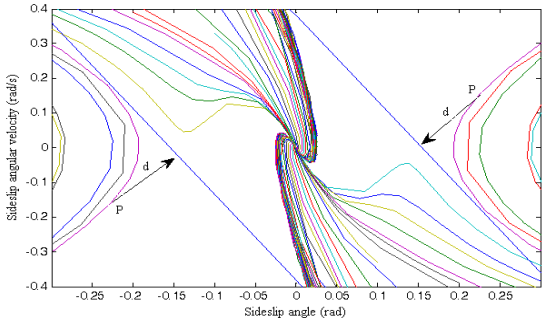

Figure 7. δ_f = 0rad, v=60km/h, μ=0.8

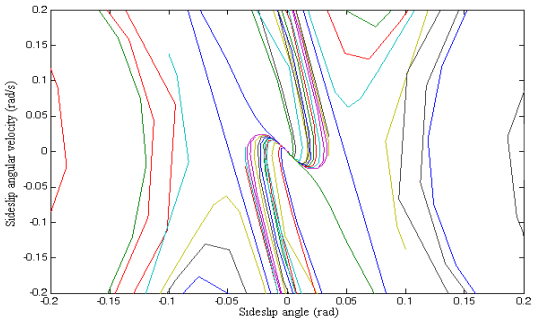

Figure 8 δ_f = 0rad, v=60km/h, μ=0.2

Figure 3-8 show that the little change of vehicle speed and front steering angle have almost little effect on the stable region. Therefore we can consider the stable region with δ_f =0rad and v=60km/h as the stationary stable region. Its boundaries can be respectively obtained by MATLAB [10], as shown in Figure 7 and Figure 8. And the expression of the straight line is as follows:

$$\left|B_1\dot{\beta}+\beta\right|=B_2 \tag{5}$$

In the stable region which is constituted by the two straight lines, all of the trajectory lines started from any initial value $\left[\beta\text{-}\dot{\beta}\right]$ finally converge to the stable node $\left[0\text{-}0\right]$. All of the nodes, $\left[\beta\text{-}\dot{\beta}\right]$, which are outside the stable region, are in an unstable state. And the expression of the corresponding stable region can be described as [11]:

$$\left|B_1\dot{\beta}+\beta\right| \le B_2 \tag{6}$$

Only when the above formula is established, the vehicle can be regarded as stable, or vice versa. And its boundaries can be respectively obtained by MATLAB, as shown in Figure 7 and Figure 8. And its boundary expressions are as the following:

$$\begin{cases} \left|0.4063\dot{\beta}+\beta\right|=0.1544 & \left(\mu=0.8, where\ B_1=0.4063 \quad B2=0.1544\right) \\ \left|0.1750\dot{\beta}+\beta\right|=0.0490 & \left(\mu=0.2, where\ B_1=0.1750 \quad B2=0.0490\right). \end{cases} \tag{7}$$

From Figure 7 and Figure 8, it is easy to find that the stable region with μ=0.8 is significantly wider than that with μ=0.2. Actually, the vehicle at low road adhesion coefficient is more prone to become unstable. We can draw a conclusion that the determination of the stable region is correct.

3.2. Design of DYC Controller

The vehicle inside the stable region can be regarded as a linear model. And the vehicle outside of the stable region is unstable, and nonlinear saturation will occur to its tires. So firstly we design DYC controller to control the nonlinear vehicle back into the stable region. The aim of DYC controller is to make the vehicle become stable from unstable state by direct yaw moment. That is to ensure that the distance d become zero. The simple PI algorithm is adopted. And the input of PI controller is the distance d, and the output signal is direct yaw moment M. The concrete control block diagram is shown in Figure 9.

It is assumed that the status point p is outside of the stable region, the nearest distance between point P and the boundary of the stable region is d, as shown in Figure 7. And the expression of d is as follows:

$$d=\begin{cases} \dfrac{\left|B_1\dot{\beta}_0+\beta_0\text{-}B_2\right|}{\sqrt{B_1^2+1}}, & \text{P is above the stable domain} \\ \dfrac{\left|B_1\dot{\beta}_0+\beta_0+B_2\right|}{\sqrt{B_1^2+1}}, & \text{P is below the stable domain.} \end{cases} \tag{8}$$

4. Design of AFS Controller based on Sliding Mode Variable Structure

AFS controller commands the front steering angle with the objective of tracking the reference sideslip and yaw rate signals corresponding to the reference vehicle handling behavior [12]. And its control objective is the tracking error between the actual sideslip angle, yaw rate and the reference ones. The concrete control block diagram is shown in Figure 10.

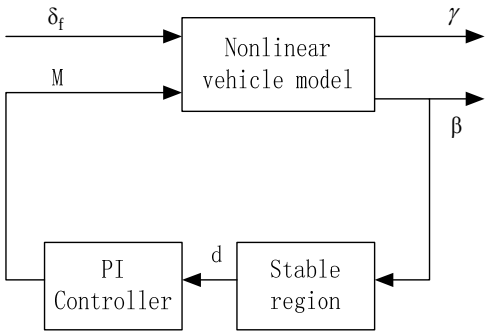

Figure 9. DYC Control Block Diagram

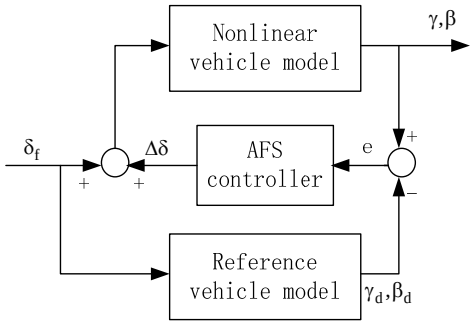

Figure 10. AFS Control Block Diagram

Assuming that the error between the actual vehicle model and the reference vehicle model is e, then:

$$\boldsymbol{e} = \boldsymbol{x} - \boldsymbol{x}_{\boldsymbol{d}} = \begin{pmatrix} \beta - \beta_d & \gamma - \gamma_d \end{pmatrix}^T \tag{9}$$

Combined with the actual vehicle model and the reference vehicle model, the error function is given below:

$$\begin{aligned} \dot{\mathbf{e}} = \dot{\mathbf{x}} - \dot{\mathbf{x}}_{\mathbf{d}} &= \mathbf{A}x + \mathbf{B}u - \left(\mathbf{A}_{\mathbf{d}}x_d + \mathbf{B}_{\mathbf{d}}u_d\right) \\ &= \mathbf{A}_{\mathbf{d}}\mathbf{e} + \mathbf{B}\left(u - u_d\right) + \left(\mathbf{A} - \mathbf{A}_{\mathbf{d}}\right)\mathbf{x} + \left(\mathbf{B} - \mathbf{B}_{\mathbf{d}}\right)\mathbf{u}_{\mathbf{d}} \\ &= \mathbf{A}_{\mathbf{d}}\mathbf{e} + \mathbf{B}\Delta u + \left(\mathbf{A} - \mathbf{A}_{\mathbf{d}}\right)\mathbf{x} + \left(\mathbf{B} - \mathbf{B}_{\mathbf{d}}\right)\mathbf{u}_{\mathbf{d}} \end{aligned} \tag{10}$$

When the latter two are ignored, the above equation can be rewritten as:

$$\dot{\boldsymbol{e}} = \boldsymbol{A}_{\boldsymbol{d}}\boldsymbol{e} + \boldsymbol{B}\Delta u \tag{11}$$

It is assumed that $\boldsymbol{s} = \boldsymbol{G}\boldsymbol{e}$, where $\boldsymbol{G} = [g_1, 1]^T$. And index reaching law, $\dot{\boldsymbol{s}} = -\boldsymbol{k}\boldsymbol{s} - \varepsilon sign(\boldsymbol{s})$ (where k, s are positive numbers), is used to ensure good dynamic quality and stability of sliding mode. If the error dynamical system is in the sliding mode, $\boldsymbol{s} = \dot{\boldsymbol{s}} = 0$. The equivalent control angle can be obtained:

$$\Delta u = \left(\mathbf{G}\mathbf{B}\right)^{-1}\left(-\mathbf{G}\mathbf{A}_{\mathbf{d}}\mathbf{e} - \mathbf{k}\mathbf{s} + \varepsilon sign\left(\mathbf{s}\right)\right). \tag{12}$$

The switching coefficient $\boldsymbol{G}$ can be solved to ensure the final sliding mode with pre-given set of poles $\Lambda = \{\lambda_i, i = 1, 2, ..., n-m\}$, through the pole placement method. Here the pre-given set of pole is $\Lambda = \{-5\}$.

5. Simulation Results and Analysis

At the constant speed of 180 Km/h, the sideslip angles and the yaw rates are obtained with $\delta_f = 0.4\sin(\pi t)$ and μ=0.8, or μ=0.2, as respectively illustrated in Figure 11-14. The direct yaw moments with DYC controller is shown in Figure 15 and 16. And the front steering angles are shown in Figure 17 and 18.

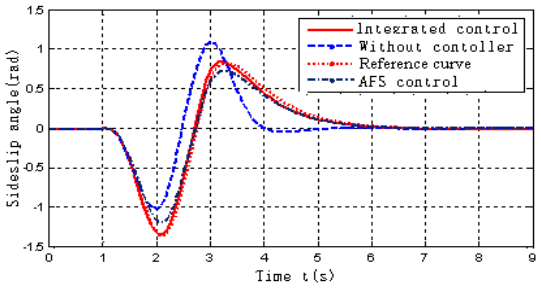

Figure 11. Sideslip Angles with μ=0.8

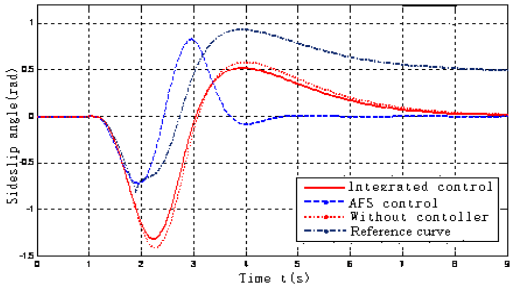

Figure 12. Sideslip Angles with μ=0.2

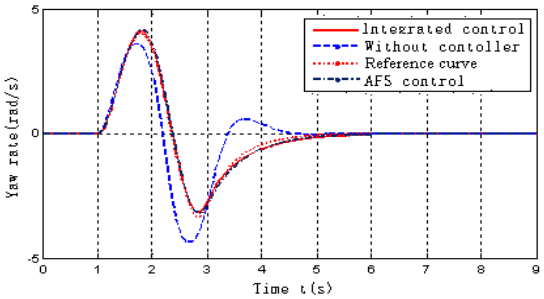

Figure 13. Yaw Rates with μ=0.8

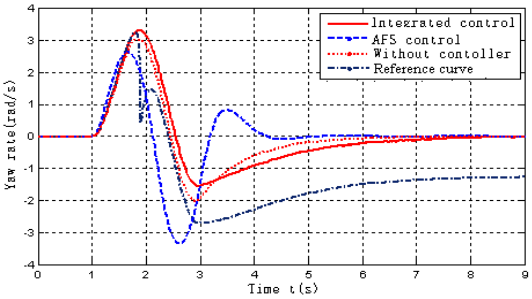

Figure 14. Yaw Rates with μ=0.2

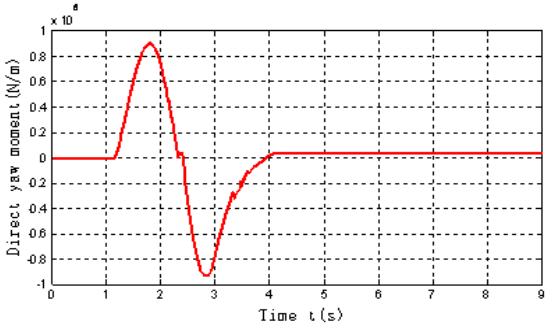

Figure 15. Direct Yaw Moments with μ=0.8

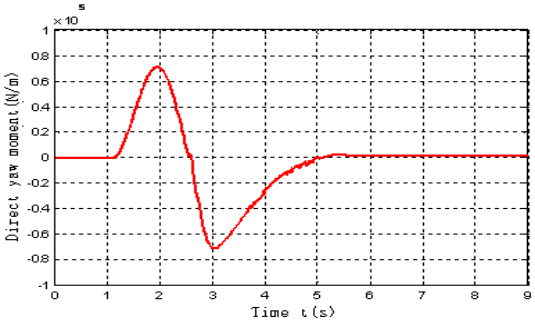

Figure 16. Direct Yaw Moment with μ=0.2

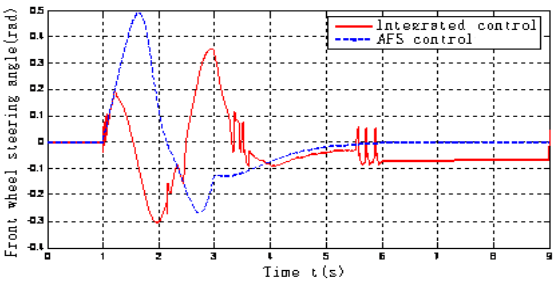

Figure 17. Font Steering Angles with μ=0.8

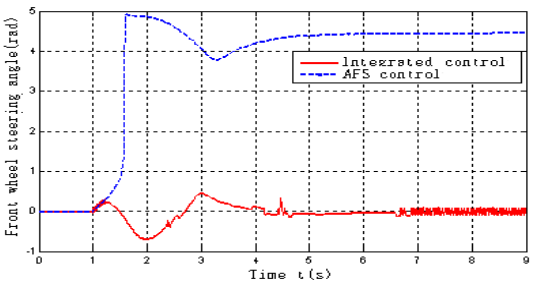

Figure 18. Front Steering Angles with μ=0.2

Figure 11 and Figure 12 show that the differences between the sideslip angle without control and the reference ones at different adhesion coefficient are large. Figure 13 and Figure 14 show that the yaw rates without controller are not coincide with the reference ones. But both of the sideslip angle and the yaw rate with integrated control of DYC and AFS can track the reference ones very well. Seen form Figure 15 and Figure 16, the direct yaw moment value with the integrated control of DYC and AFS in the high adhesion coefficient road is 90KN, While in

the low adhesion coefficient road, 70KN. Figure 17 shows that in the high adhesion coefficient road, the front steering angle with AFS controller is 0.5rad (28.7°), and the front steering angle with integrated control of DYC and AFS is 0.35rad (20°). Figure 18 shows that in the low adhesion coefficient road the front steering angle with integrated control of DYC and AFS is 0.5rad (28.7°), and the front steering angle with AFS controller is 5rad (287°), which is obviously far beyond the allowed maximum angle of the steering mechanism. That is to say that the integrated control can greatly reduce the front steering angle, which can be realized by the steering mechanism.

So we can draw a conclusion that that the integrated control of DYC and AFS has more advantages, which can not only make the sideslip angle and the yaw rate track the reference values, but also ensure the front steering angle to be realized by the steering mechanism.

6. Conclusion

Vehicle stable region is firstly determined by phase plane method. DYC controller and AFS controller have been successfully designed. And the vehicle handling stability has been improved by the integrated DYC and AFS controller. However the integrated DYC and AFS controller can make the sideslip angle and yaw rate track the reference values very well. It shows that the input of direct yaw moment can improve the tires nonlinear saturation problem, and reduce the output of the front steering angle, especially in the low adhesion coefficient road. The control effect of the integrated DYC and AFS controller is obvious and it can ensure the effective work of the steering mechanism. More complex vehicle models can be established in the future to further verify the effectiveness of the integrated control.

Acknowledgements

This work is supported by National Natural Science Fund Project (No.11272159), Natural Sciences Fund Project of Jiangsu Province universities and colleges (No.08KSD580049) and Technological Innovation Fund Project of Nanjing Forestry University (No.163106007).

References

[1] Trachtler A. Integrated vehicle dynamics control using active brake, steering and suspension systems. *International Journal of Vehicle Design*. 2004; 36(1): 1-11.
[2] Goodarzi A. Alirezaie M. Integrated fuzzy/optimal vehicle dynamic control. *International Journal of automotive technology*. 2009; 10(5): 567-575.
[3] Jie Tian. Research on Dynamic Analysis and Control Method of Steer-by-wire System for Vehicle. PhD Thesis. Jiangsu University; 2011.
[4] Kitajima K, Peng H. *Hinf control for integrated sideslip, roll and yaw controls for ground vehicles*. Proceeding of AVEC'2000, Michigan. 2000: 63-72.
[5] Shibahata Y, Shimada K, Tomari T. Improvement of vehicle maneuverability by direct yaw moment control. *Vehicle System Dynamics*. 1999; 22: 465-481.
[6] Van Zanten AT, Erhardt R, Pfatt G, et al. *Control aspects of the Bosch-VDC.* AVEC'96 International Symposium on Advanced Vehicle Control, Aachen. 1996: 574 -607.
[7] E Ono, S Hosoe, S Doi, et al. Theoretical approach for improving the vehicle robust stability and manuverbility by active front wheel steering control. *Vehicle system dynamics*. 1998; 28: 748-753.
[8] Pacejka HB, Sharp RS. Shear Force Development by Pneumatic Tires in Steady State Conditions: A Review of Modeling Aspects, Vehicle System Dynamics. *International Journal of mechanics and mobility*. 1991; 20(3-4): 121-175.
[9] Eiichi Ono, Shigeyuki Hosoe, Hoang D, et al. Bifurcation in Vehicle Dynamics and Robust Front Wheel Steering Control. *IEEE Transactions on Control System Technology*. 1998; 6 (3): 412-420.
[10] Inagaki S, Kshiro I, Yamamoto M. Analysis on vehicle stability in critical cornering using phase-plane method. *JSAE Review*. 1995; 16(2): 287–292.
[11] Deping Wang, Konghui Guo. Vehicle Dynamics Control stability control principle and control strategy. *Mechanical Engineering*. 2000; 43(3): 97-99.
[12] Qidong Wang, Guihua Zhang, Wuwei ChenJie. Based on sliding mode variable structure control of vehicle dynamics stability control study. *Chinese Mechanical Engineering*. 2009; 20(5): 622-625.